International Journal of
INTELLIGENT SYSTEMS AND APPLICATIONS IN ENGINEERING

ISSN : 2147-6799 www.ijisae.org Original Research Paper

Design of Torque and Power Density Improvement According to the Rotor Shape of IPMSM

Chung-Ho Lee[1], Hong-Rae Noh[2] and Ki-Chan Kim[3*]

Submitted: 08/11/2022 **Accepted:** 10/02/2023

Abstract: In the case of Interior Permanent Magnet Synchronous Motor (IPMSM), it refers to a motor with a structure in which permanent magnets are embedded in the rotor core. Since the permanent magnet has a very low permeability compared to the permeability of the air gap and the magnetic permeability of the Rotor core, the effective air gap of the magnetic flux, depending on the relationship between the d-axis, which is the axis in which the magnetic flux is concentrated, and the q-axis, which is electrically 90degrees ahead of the d-axis, q. In order to reduce the amount of magnetic flux leaking from the shaft, the thickness of the rotor rib is modified and the characteristics are compared according to the experiment.

Keywords*: Interior Permanent Magnet Synchronous Motor (IPMSM), Rotor Rib, Barrier, Torque, Power Density, Finite Element Analysis (FEA), Fiber Reinforced Plastics (FRP)*

1. Introduction

In the case of IPMSM, it refers to a motor with a structure in which permanent magnets are embedded in the rotor core, and there is no need for additional devices to prevent the scattering of permanent magnets during rotation, as in the case of a Surface Permanent Magnet Synchronous Motor (SPMSM) [8][9][11][13]. However, in order to embed permanent magnets in the rotor core, various types of barrier halls are dug to embed permanent magnets [6][7][14][15]. At this time, since the permanent magnet has very low permeability compared to the permeability of the air gap and the magnetic permeability of the rotor core, the effective air gap of the magnetic flux path changes depending on the rotor position [2][12]. In this paper, in order to improve the power density and torque by increasing the concentration of magnetic flux, the thickness of the rotor rib is modified to reduce the amount of magnetic flux leaking from the d-axis in the direction where the magnetic flux is concentrated and the q-axis electrically 90 degrees ahead of the rating [4][10]. At speed, Finite Element Analysis (FEA) is performed to conduct a characteristic comparison experiment.

2. Basic Model Properties

This paper conducts an experiment by selecting a rotor barrier shape as Single V-type, Double V-type, and Delta-type to clearly examine the difference between torque and power density depending on Rib length and effective airgap length based on three types of IPMSM [1][3][5].

Figure 1 below presents the models of the Single V-type, Double V-type and Delta-type.

[1, 2]*Master's Course in Electrical Engineering, Hanbat National University, Daejeon- 34158, Korea*
[3]*Professor, Department of Electrical Engineering, Hanbat National University, Daejeon- 34158, Korea*
[3*]*kckim@hanbat.ac.kr*

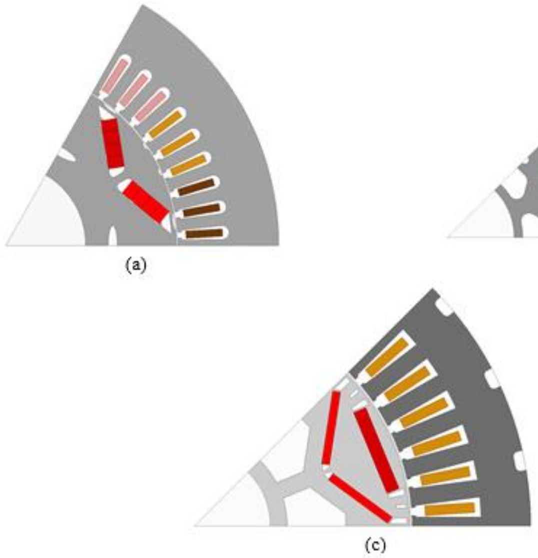

(a) Single V-type **(b)** Double V-type **(c)** Delta-type

Fig 1. Model before removing the Rib according to the shape of the Barrier.

In order to minimize the leakage magnetic flux on the q-axis, the experiment is conducted in a direction to increase the length of the effective airgap by reducing the thickness of the Rib. In addition, we compare each Basic model according to the Barrier shape without removing the Rib with the improved model by removing the Rib.

Table 1 below shows the characteristics of each Basic model according to the shape of the Barrier.

Table 1. Basic characteristics of each model according to the shape of the barrier.

	Single V-type	**Double V-type**	**Delta-type**	**Unit**
Number of Poles / Slots	6 / 54	8 / 72	8 / 48	-
Rib Length	0.95	2.00	0.80	mm
Airgap Length	0.80	1.00	0.75	
Stack Length	134	201	140	
Stator External Diameter	240	350	200	
Rotor External Diameter	150	224	128	
Rotor Internal Diameter	70	85	45.1	

The experiment is conducted in the order of Single V-type, Double V-type, and Delta-type, and Finite Element Analysis (FEA) is performed at the Rated speed to determine the degree of magnetic flux saturation and leakage in the q-axis near the Rib of each model. Torque, Efficiency, and Power Density at the Rated speed of each model before removing the Rib are shown in Table 2 below, and Figure 2 illustrates the Magnetic flux density and Magnetic flux diagram.

Table 2. Characteristics at Rated Speed according to model before Rib removal.

	Single V-type	**Double V-type**	**Delta-type**	**Unit**
Base Speed	5,230	1,600	3,350	rpm
Torque	440.15	1,802.7	285.5	Nm
Output	241.06	302.05	100.16	kW
Efficiency	92.83	92.86	95.52	%

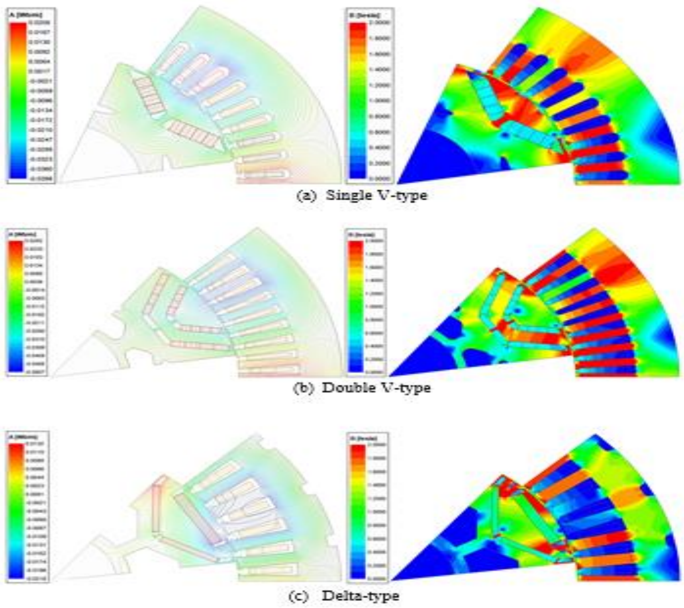

Fig 2. Magnetic flux density and Magnetic flux diagram for each model.

As may be seen from Figure 2, models commonly have magnetic fluxes moving between the Rotor and the Stator through the vicinity of the Rib, but a large amount of leakage magnetic flux is generated, thereby leading to excessive saturation. Therefore, in order to reduce saturation due to leakage magnetic flux by increasing resistance compared to the Rotor core near the Rib, the FEA is carried out by removing the Rib from the existing Rotor core.

3. Frp Applied Model Properties

In the previous experiment, the shape of the Rotor core was modified by removing the Rib to increase the resistance compared to the Rotor core and reduce the leakage magnetic flux near the Rib. If the Rib is removed in this way, the Rotor core is separated into several pieces, so something is needed to hold it like the existing Rotor core shape.

At this time, Fiber Reinforced Plastics (FRP) with high strength compared to low weight are selected to hold the Rotor core even in an area that rotates at high speed without magnetically affecting it.

The basic characteristics of each model presented in Table 1 are maintained, the Rib is removed, the FRP is wrapped around the Rotor core, and the shape of each model's Rib removed is presented in Figure 3 below.

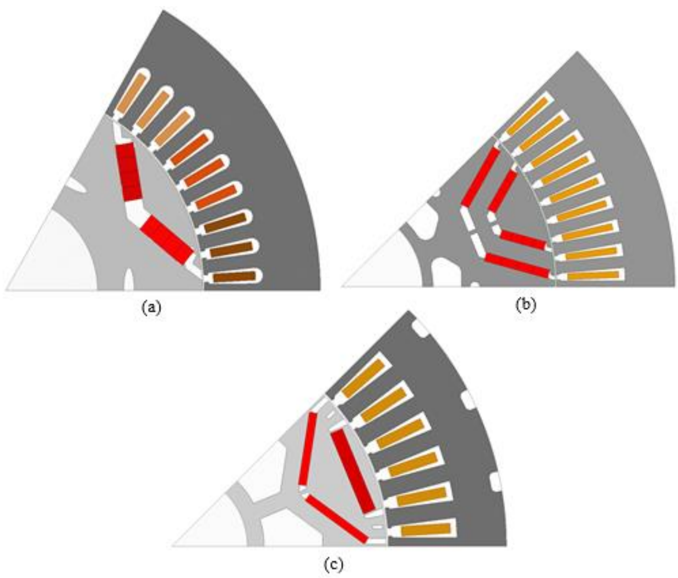

(a) Single V-type **(b)** Double V-type **(c)** Delta-type

Fig 3. Model with FRP applied Rib removed.

Remove the Rib from each model, wrap the rotor core with the FRP, and conduct FEA to check the magnetic flux density and magnetic flux diagram to confirm that the leakage magnetic flux is reduced near the existing Rib. By removing the Rib, it can be used less than the existing iron amount in the Rotor core, and the Torque and Power Density are improved when a command value such as the existing model is applied due to a decrease in leakage magnetic flux.

Figure 4 below shows the magnetic flux density and magnetic flux diagram of each model with Rib removed, and when the same command value is applied in Table 3, it is compared with the existing model and the improvement model.

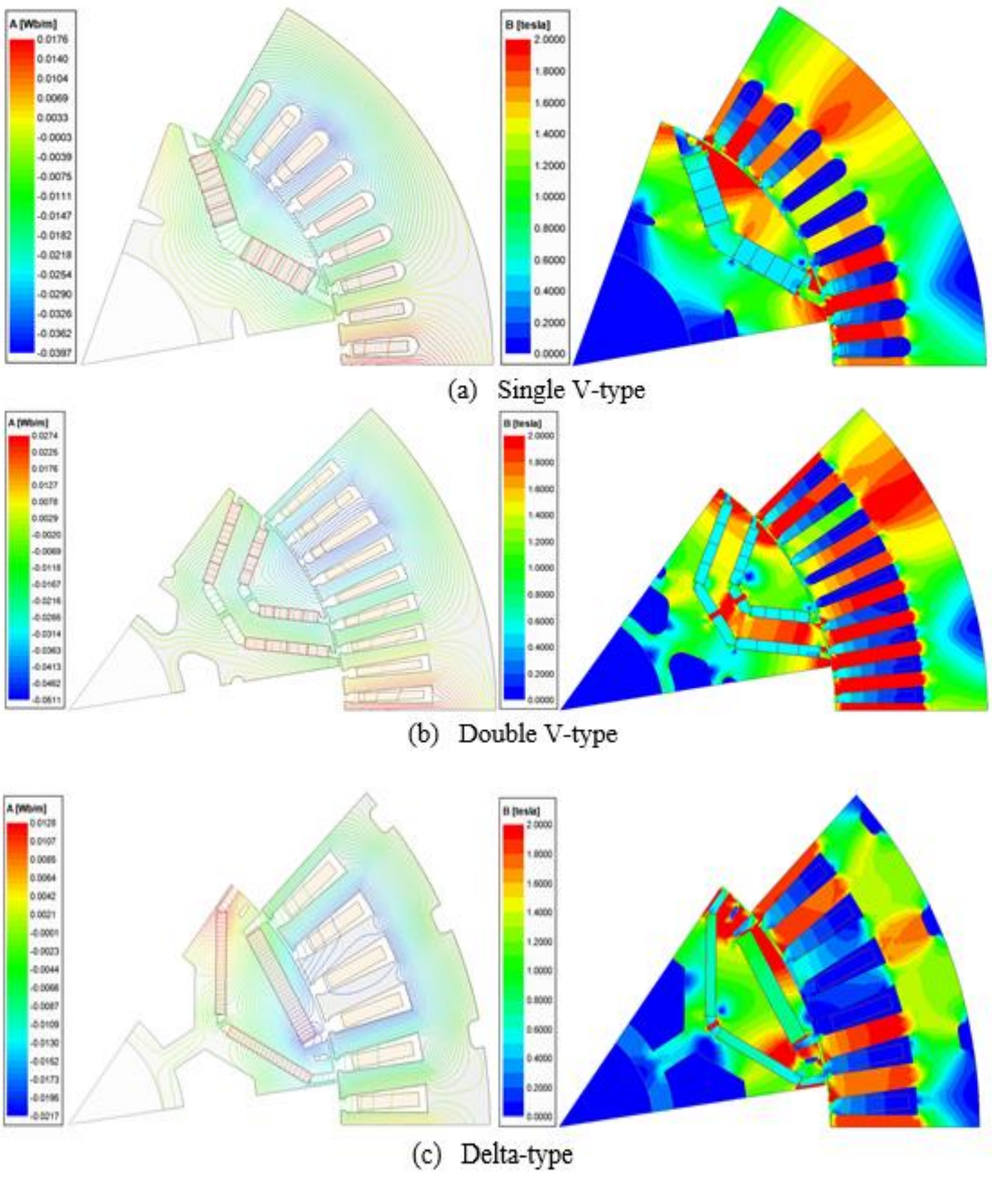

Fig 4. The magnetic flux density and magnetic flux diagram of each model with the Rib removed.

Table 3. Comparison of characteristics with existing models when applying the same command value.

	Single V-type		**Double V-type**		**Delta-type**		**Unit**
	Using Rib	**Remove Rib**	**Using Rib**	**Remove Rib**	**Using Rib**	**Remove Rib**	
Base Speed	5,230		1,600		3,350		rpm
Current	921		792		358		A

Current Angle	57		55.3		44		deg
Torque	440.15	473.84	1,802.70	1,862.33	285.50	297.42	Nm
Power	241.06	259.51	302.05	312.04	100.16	104.34	kW
Weight	11.34	11.17	37.74	37.51	7.29	7.22	kg
Power Density	21.26	23.23	8.00	8.32	13.74	14.45	kW/kg

4. Conclusion

In this paper, the degree of improvement in Torque and Power Density during Rib removal was analyzed through FEA for three types of barrier shapes most commonly used in IPMSM.

By removing the Rib, the leakage magnetic flux of the q-axis generated near the Rib was reduced, resulting in improved Torque and Efficiency, and even improved Power Density.

By enclosing the FRP around the Rotor, it is necessary to prevent the scattering of the Rotor core in the high-speed area, but FRP is not a problem with fiber-reinforced plastics, which are not magnetic materials. As the iron in the Rotor core is also reduced, the cost of fabrication is expected to be further reduced.

As a result, Torque and Power Density improved by 7.65 [%] and 17.42 [%] on IPMSM of Single V-type, 3.31 [%] and 3.56 [%] on IPMSM of Double V-type, and 4.18 [%] and 4.49 [%] on IPMSM of Delta-type, respectively.

5. Acknowledgements

This work was supported by the Technology Innovation Program (20011435, Development of largecapacity Etransaxle and application technology of 240kW class in intergrated rear axle for medium and large commercial vehicles) funded By the Ministry of Trade, Industry & Energy(MOTIE, Korea)

This work was supported by the Korea Institute of Energy Technology Evaluation and Planning(KETEP) and the Ministry of Trade, Industry & Energy(MOTIE) of the Republic of Korea (No. 20204030200080).

References

[1] Chakraborty, Shivam, Sandeep V. Nair, and Kamalesh Hatua. "Effect of v angle variation and strengthening rib on performance characteristics of ipmsm motor for electric vehicles." 2021 1st International Conference on Power Electronics and Energy (ICPEE). IEEE, 2021.

[2] Lumertz, Mateus Moro, et al. "Design of IPMSM with Reduced Torque Ripple Through Advanced Sine-Shaped Poles." 2020 2nd Global Power, Energy and Communication Conference (GPECOM). IEEE, 2020.

[3] Hong, Chan-Hee, et al. "Characteristic analysis of Spoke-type IPMSM corresponding to the rib structure." 2014 17th International Conference on Electrical Machines and Systems (ICEMS). IEEE, 2014.

[4] Lim, Ho-Kyoung, et al. "Magnetic circuit design of IPMSM to improve maximum power in the field weakening region." Digests of the 2010 14th Biennial IEEE Conference on Electromagnetic Field Computation. IEEE, 2010.

[5] Lim, Ho-Kyoung, et al. "A study on the relation between rotor rib and maximum power of IPMSM in flux weakening region." 2010 International Conference on Electrical Machines and Systems. IEEE, 2010.

[6] Okamoto, Junka, et al. "Influence of magnet and flux barrier arrangement for IPMSM with concentrated winding." 2013 IEEE 10th International Conference on Power Electronics and Drive Systems (PEDS). IEEE, 2013.

[7] Pan, Zhicheng, Kai Yang, and Xiaojie Wang. "Optimal design of flux-barrier to improve torque performance of IPMSM for electric spindle." 2015 18th International Conference on Electrical Machines and Systems (ICEMS). IEEE, 2015.

[8] Sieklucki, Grzegorz. "An investigation into the induction motor of tesla model S vehicle." 2018 International Symposium on Electrical Machines (SME). IEEE, 2018.

[9] Thomas, Robin, et al. "Modeling and design analysis of the Tesla Model S induction motor." 2020 International Conference on Electrical Machines (ICEM). Vol. 1. IEEE, 2020.

[10] Laskaris, Konstantinos I., and Antonios G. Kladas. "Permanent magnet shape optimization for high efficiency electric traction motors." Digests of the 2010 14th Biennial IEEE Conference on Electromagnetic Field Computation. IEEE, 2010.

[11] Thomas, Robin, et al. "Comparative study of the Tesla Model S and Audi e-Tron Induction Motors." 2021 17th Conference on Electrical Machines, Drives and Power Systems (ELMA). IEEE, 2021.

[12] Baek, Sung-min, Gyu-won Cho, and Gyu-tak Kim. "The Design of Iron Loss Minimization of 600W IPMSM by Quasi-newton Method." The Transactions of The Korean Institute of Electrical Engineers 66.7 (2017): 1053-1058.

[13] Murakami, Hiroshi, et al. "The performance comparison of SPMSM, IPMSM and SynRM in use as air-conditioning compressor." Conference Record of the 1999 IEEE Industry Applications Conference. Thirty-Forth IAS Annual Meeting (Cat. No. 99CH36370). Vol. 2. IEEE, 1999.

[14] Du, Jingjuan, Xiaoyuan Wang, and Haiying Lv. "Optimization of magnet shape based on efficiency map of IPMSM for EVs." IEEE Transactions on Applied Superconductivity 26.7 (2016): 1-7.

[15] You, Yong-Min. "Shape Optimization of PMSM Based on Automated Design of Experiments and Multi-layer Perceptron." Journal of Next-generation Convergence Technology Association 4.5 (2020): 478-484.